CONEM 2016
CONGRESSO NACIONAL DE ENGENHARIA MECÂNICA
21 - 25 AGOSTO DE 2016
FORTALEZA - CEARÁ

COMPUTATIONAL MODELING AND ANALYSIS FOR AN AUTOMOTIVE SUSPENSION SYSTEM WITH NONLINEAR DAMPING CURVES IMPORTED FROM AN EXTERNAL DATABASE

Código:
CON-2016-1333

Abstract: *This paper aims to numerically modelate in MATLAB the vertical behavior of a high performance vehicle suspension system, identifying the best setting for the dampers based on its dynanometric characteristics curves. For this reason, a quarter car model with two degrees of freedom was developed according to differential equations obtained from the free-body diagram of the prototype sprung mass and unsprung mass. The final computational numerical code allows to automatic import the component characteristics curves from an external database. However, due the nonlinearity and asymmetry of its cuvers, intermediary calculations are perfomed to define the instantaneous damping constant based on the momentaneum base excitation applied, resulting in a easy way to identify the time-domain system response. Furthermore, filters are implemented to the numerical code due the high number of possible inputs, identifying automatically potential variables to the project. During the analysis of the kinematic response for each of the vehicle masses in different road inputs the particular and homogeneus solutions are analysed individually in order to identify the influence of each damping curve in each motion state. This response analysis highlights the use of 59% of the design nominal stroke, and peaks on the sprung mass vertical acceleration that exceed 3g, as well as operational velocities that exceed its maximum velocity limit. The final proposed solutions shown a compromise between reducing the relative displacement between the masses and a small time window to minimize the dynamic negative effects in each maneuver.*

Key-words: *MATLAB, Non-linear Damping, Vehicle Dynamics, Quarter-car Model, External Databse.*

1. INTRODUCTION

The applicability of computational models to predict and enhance the response of automotive suspension systems is gradually being explored in order to improve the handling and the overall performance of prototypes. Therefore, the convergence between the simulation results and physical tests is a highly desirable feature since it minimizes test time and design cost. Smith (1978) highlights the compromise between the optimization of an automotive system and the driver preferences/sensibility. However, Harty (2009 Apud Cristiano, 2011) states that the increment in complexity and number of details tends to reduce the model efficiency due to the limited reliability of tires mathematical models.

A solution to the scenario is to use simplified models and adapt it to specific boundary conditions of each project. For instance, Fernandes (2015) describes the behavior of a passenger’s vehicle wheel with nonlinear and asymmetric damping during the bump and rebound, considering some kinematics of the physical components. Nevertheless, Freitas (2006) compares the vertical response on time-domain and frequency-domain of a MacPherson vehicle suspension system, modeled in multibody on ADAMS MSC Software, to a quarter car model with two GDL, modeled in MATLAB, highlighting the similarities of both system to describe the suspension oscillatory behavior. Furthermore, these simplifications enable the suspension response regarding the comfort, variations in the normal forces developed on the tire and the forces transmitted to the frame, as stated by the review performed for Crolla and Sharp (1987 apud Freitas, 2006).

1.1. Project objectives

Determinate potential configurations settings among the dynamometric damper curves for an Öhlins TTX25 MkII utilized in a Formula Student prototype based on computer modeling and simulation performed in MATLAB.

1.1.1. Theme delimitation and justification

The project analyses the dampers based in a quarter car model with two degrees of freedom (DOF), blocking the remaining variables. The dynamometric damper curves analyzed are only curves provided by the manufacturer, disregarding any further internal adjustments performed by the operator. These assumptions aim to reduce the number of input conditions in order to prioritize the decision making process to variables with great influence on the overall prototype performance, providing project guidelines.

The rules of the 2015 Formula Student, in which the vehicle compete, state that prototypes that do not show high integrity in regard to the driver safety are subject to immediate disqualification of the dynamic tests. Therefore, since the dampers are directly related to the forces developed between the tire and the road, a malfunction of these components compromises the performance and safety of the prototype. Moreover, the correct use of dampers ensures better performance and consequently higher score.

1.2. Design variable details

The real prototype uses a pull road suspension system on the front axle and a push road suspension system on the rear axle, triggering through a rocker arm the dampers and coil springs f/r (32/42)kN.mm^{-1} fixed on the frame. These two systems are independent and substantially isolate the motion of each wheel. The suspension arms are asymmetrical and converging forming a double A in order to control the negative effects of its kinematics. Each axle has a torsion spring that controls the sprung roll, limiting the sensitivity roll to 1.1°/g and the negative effects of lateral load transfer. The static normal load distribution is 50% on each axis, improving the longitudinal forces production, the brake control, and the handling. The adhesion is ensured by Hoosier tires with different aspect ratios and different internal pressure on each axle, which combined to the springs gives to the prototype an oversteer behavior and natural frequencies of f/r (3.15/3.30)kN.mm^{-1}.

The real prototype has four Öhlins TTX25 MkII FSAE dampers as shown in Figure 1. The component is the hydraulic type with double tube, only sensitive to the internal piston speed. However, their characteristic curves may be changed by means of intermediary valves between a nitrogen gas chamber and the main cylinder. These valves regulate the gas pressure drop to the main cylinder, as well as the pressure drop between the main cylinder and the nitrogen cylinder, allowing different operational behavior during compression and extension of the piston. Furthermore, each of these valves also allows adjustments for high and low speed operation. These characteristics combined to the wide range of available damping coefficients make this damper model excellent for use in FSAE applications.

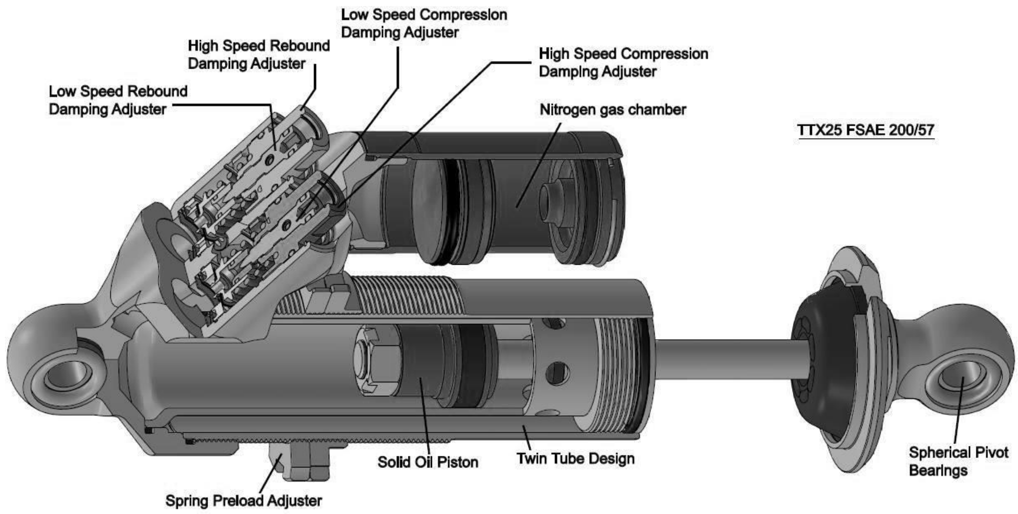

Figure 1. Öhlins TTX25 MkII FSAE computational aided design model

2. NUMERICAL MODELING

2.1. Generic quarter car model

Any system must have the same number of equations of motion that the number of GDL that compose it in order to enable mathematical models to predict it response in a delimited range. In addition, the system will feature the same number of natural frequencies than the number of general coordinates that compose it. Therefore, the two GDL that composes the quarter car model are based on the suspended and unsuspended masses with different motions as shown in Figure 2.

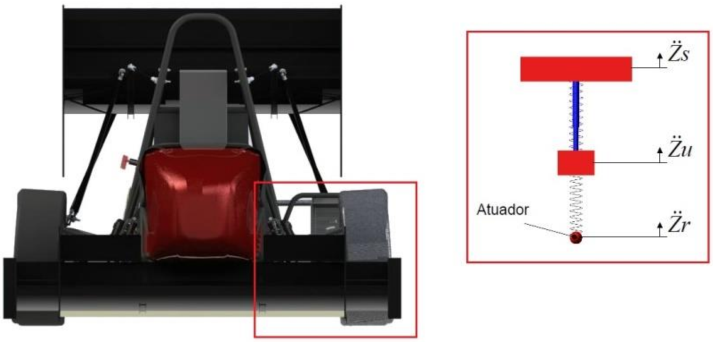

Figure 2. Inputs and outputs of the generic quarter car model.

The differential equations that describe the dynamic behavior of a quarter car model are obtained applying Newton's second law in a free body diagram related to each vehicle mass. The suffixes "s" and "u" indicates that the component belongs to the sprung mass and unsprung mass, respectively. Since each of the masses has isolated motions, Equation 1 is used to represent the sprung mass response and Equation 2 for the unsprung mass response.

$$M\ddot{Z} + C_S\dot{Z} + K_S Z = C_S\dot{Z}_u + K_S Z_u + F_b \tag{1}$$

$$m\ddot{Z}_u + C_S\dot{Z}_u + (K_S + K_t)Z_u = C_S\dot{Z} + K_S Z + K_t Z_r + F_w \tag{2}$$

2.1.1. Normative coordinate system

The Cartesian coordinate system adopted in this paper follows the European standard ISO 4130: 1978 (ISO 4130: 2007), which defines the vehicle Center of Gravity (CG) as the origin of the axes. The normal and rotational motion about each axis are defined as shown in Figure 3.

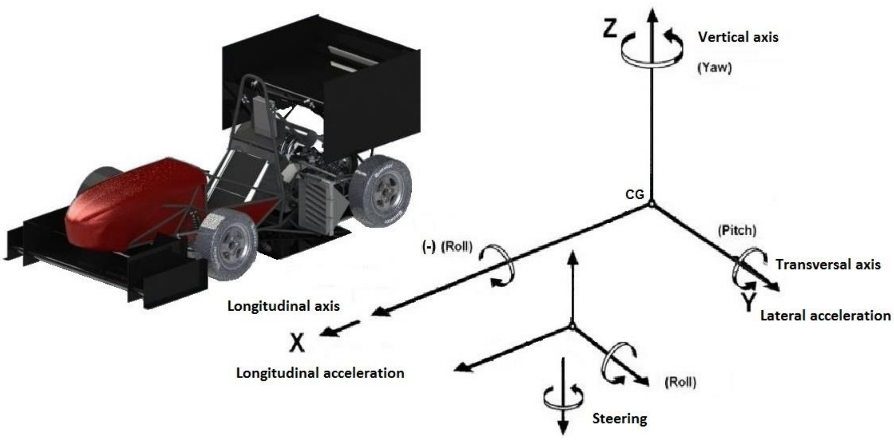

Figure 3. Cartesian coordinate system based on the European standard ISO 4130:1978

2.2. Numerical model implementation

The numerical model in MatLab is based on the sequence of operation shown in Figure 4. In its first step, the invariable boundary conditions as the components stiffness and mass, and the longitudinal speed of the vehicle are introduced. In addition to this inputs, a vector *tspan* is introduced to stablish the beginning and the end of the simulation, as well as the resolution in which the calculations are performed. Furthermore, the initial conditions for the simulation also should be established at this stage in order to calculate the response after the first time step. Therefore, the following vector is introduced to define the position and velocity of each mass according to its label, and for this specific case the both masses are in the neutral state.

```
z0 = [ 0; 0; 0.; 0.]; % x0 = [zMs; dzMs/dt; zMu; dzMu/dt];
```

The simulation uses an open loop processing in which an road input $Z_r(t)$ is responsible for stimulate the suspension system. The pulse is modeled aiming to represent a real maneuver in which the steering angle is varied as a function of time, because due its inherent limitations the quarter car model is not directly responsive to any steering angle variation. The first pulse input is a sinusoidal base motion, which allows identifying the particular and homogenous system response. The second pulse input consists of a positive base slope with a linear increment, followed by a flat stretch and then a negative slope with a linear decrement, which allows evaluating the system transient behavior reproducing a fast change on the steering wheel position. The position of the obstacle is converted into time through Table 1, and its vertical position $Z_r(t)$ is calculated in the system response function (Section 2.2.1.).

Table 1. Conversion from linear position into time.

Linear dimension (m)	Description	Conversion into time	Time elapsed
L1 = .1;	Road level	Dt(1) = L1/v;	t1=Dt(1)
L2 = .3;	Positive inclination	Dt(2) = L2/v;	t2=t1+Dt(2)
L3 = .2;	Plane	Dt(3) = L3/v;	t3=t2+Dt(3)
L4 = .3;	Negative inclination	Dt(4) = L4/v;	t4=t3+Dt(4)
h = .02032;	Obstacle height	Dt(1) = L1/v;	t1=Dt(1)
		Dt(2) = L2/v;	t2=t1+Dt(2)

Next, the data to be analyzed, located in an external database, is connected to the main numerical code. Furthermore, the numbers of different suspensions settings to be simulated for each one of the maneuvers are stated at this stage, which for this case are seven dynamometric damper curves with very distinct behavior. More details about these configurations are informed in Section 2.1.1.

With these set of parameters the simulation loop can be started. At this stage each of the characteristic damping curves is imported and simulated individually, and each result is saved by the *fprintf* command. Therefore, an arbitrary characteristic curve will undergo through a given excitation, and its response will be computed and subsequently analyzed and filtered in the final stage of the flowchart.

The simulation for an arbitrary curve is performed externally to the main code in a vector [t, x], which uses solver based on Rouge-Kutta methods for solving differential equations of first order. The *ode23* command uses the combination of the second and third order Runge-Kutta method, while the *ode45* command is based on the combination between the fourth and fifth order of the same method. This vector connects the input data from the main model to a function used to calculate the response according to the code below.

```
[t, x] = ode23(@df2gdl_rampa, tspan,x0, ' ', vc, fc, m_s, m_u, k_s, k_t ,t1,t2,t3,t4,h); % Ode23 solver.
```

2.2.1. Response function

The response function performs a series of calculations related to the main code. In it stage, the model data is imported through a vector *function f* that uses the vector values [t, x] according to the following code.

```
function f = df2gdl_rampa (t, x, u, fc, ms, mu, ks, kt, t1, t2, t3, t4, h) % Response function
```

The instantaneous position of the base is calculated by converting the time elapsed in height, which one consists in the simulated system excitation source. The Equation 3 illustrates the logic used for this conversion.

$$\begin{cases} t < t_1 : z(t) = 0 \\ t \geq t_1, t < t_2 : z(t) = h*(t-t_1)/(t_2-t_1) \\ t \geq t_2, t < t_3 : z(t) = h \\ t \geq t_3, t < t_4 : z(t) = h*(t_4-t)/(t_4-t_3) \\ t \geq t_4 : z(t) = 0 \end{cases} \tag{3}$$

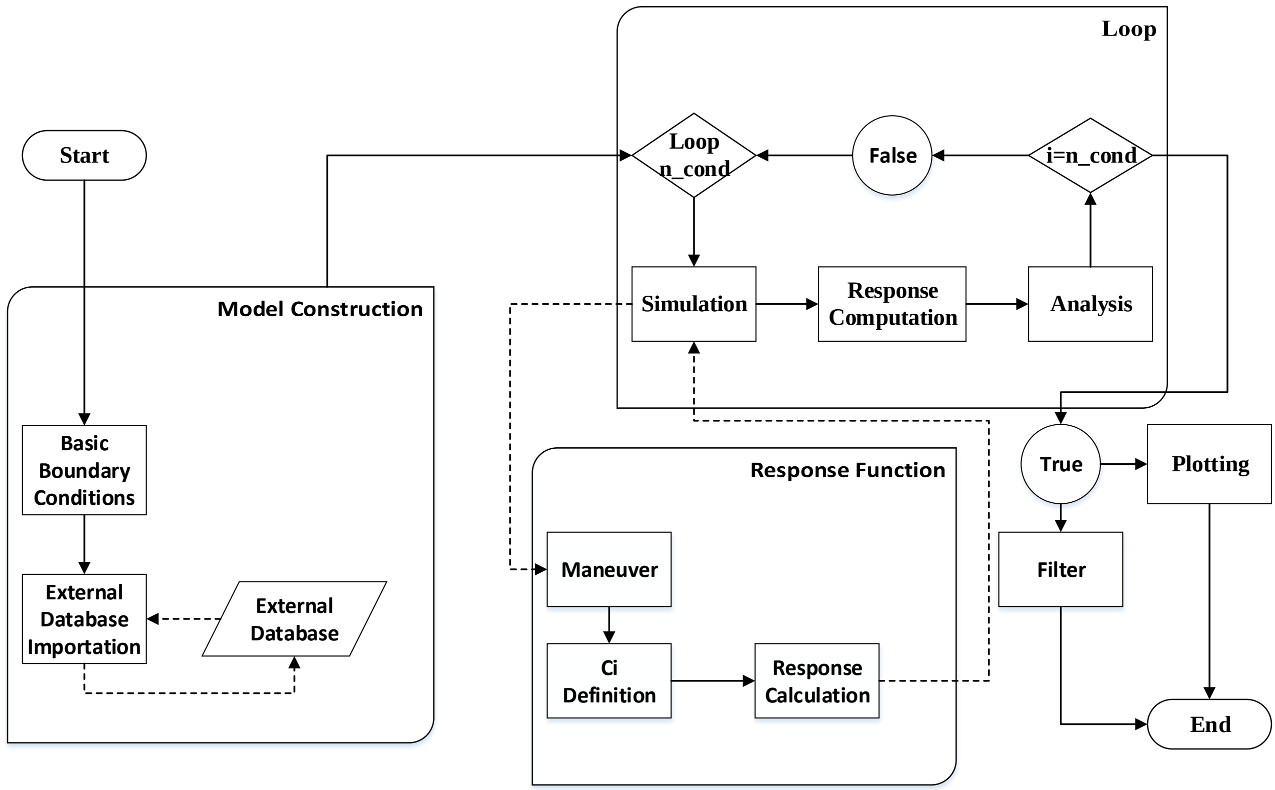

Figure 4. Simulation Flowchart.

The characteristic damping curves transformed into bijective functions and then discretized, enabling to consider as a constant the damping coefficient in a given range of velocities. In other words, each deflection point in the curves of the Figure 5 were determined and then saved in a spreadsheet. These txt documents were then saved in a common directory, consisting of the external database which one was previously imported to the MATLAB main code. Therefore, for a numeral evaluation each damper curve is consider as an array of two columns, velocity and force, with the number of rows equal to the number of deflection points of the given curve.

On the damping curves plot, the force exerted is related to velocities that vary between -255.52mm.s^{-1} and 255.52mm.s^{-1}, indicating the component working range according to Figure 5. These data are obtained on dynamometers and its damping coefficients are calculated using the first derivative of each curve as shown in Equation 4. Therefore, at time intervals at which force can be described by a first degree function in relation to the component velocity, the damping coefficient is constant. The following lines of code are implemented in the system response function to determine the instantaneous damping coefficient for each curve along *tspan*.

$$\frac{dF}{dv} = \frac{\Delta F}{\Delta v} \tag{4}$$

The force gradient is greater close to the ordinate axis. This indicates a high damping coefficient at low compression and extension speeds, suggesting that the neutral position of the suspension masses are restored in a shorter time interval when excited at low frequency. In other hand, in high operation velocity the damping coefficient is relatively lower, improving the isolation of the sprung mass. The tires where modeled based on the Kelvin-Voigt model, considering only its vertical stiffness.

The differential equations of motion can be expressed as a linear system with two first order ordinary differential equations. This formulation allows defining an equation that only depends of the suspension and road inputs, simplifying the parameterization of an arbitrary maneuver and allowing it to be implemented on the numerical code.

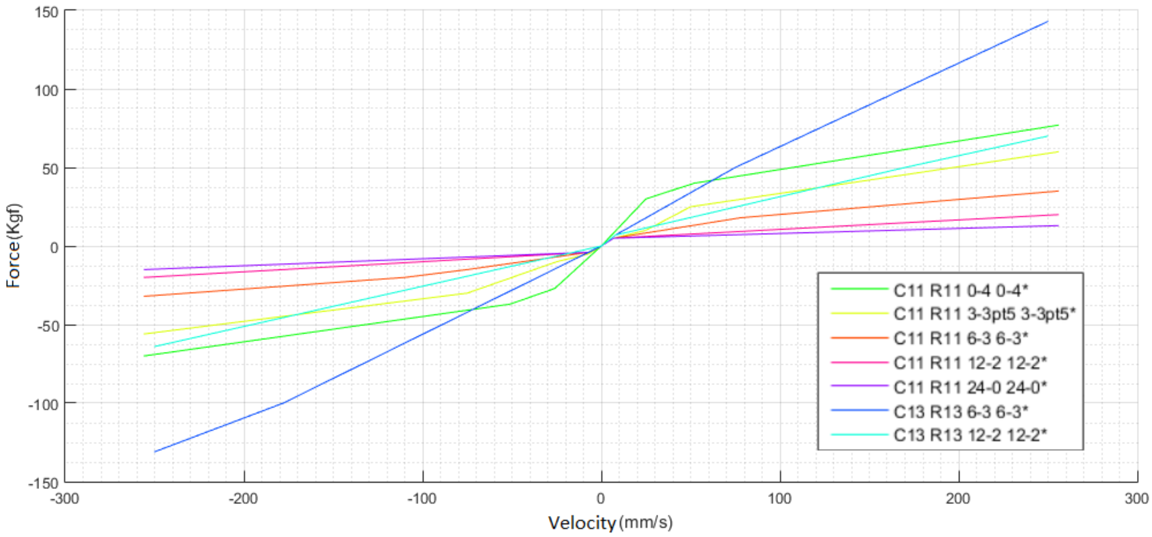

Figure 5. Damping characteristic curves used on the graphical analysis.

3. RESULTS AND DISCUSSION

The maximum stroke for the simulated dampers must be in accordance with the suspension travel limits stipulated in the project in order to avoid using the auxiliary torsions springs. Furthermore, on vehicles with a motion ratio (displacement between the wheel center and the road/ displacement between the frame and the road) 1:1, the variation on the system static position is directly related to changes in the characteristic angles of the suspension geometry, such as camber and kingpin inclination - KPI, which are not quantified in the quarter car model, but have influence on the prototype behavior.

During the ramp maneuver defined in Equation 3, the shock absorber operates within the design limits as shown in Figure 6. However, only 59% of the stipulated maximum stroke is used. The maximum positive displacement occurs on the CDC C11 R113-3pt5 3-3pt5*, reaching a peak value of 6,65mm (t = 0,1692s) after the end of the obstacle due inertia associated with system masses. The maximum negative stroke occurs on the CDC C13 R13 12-2 12-2*, reaching its peak value of 14,99mm (t = 0,2436s) after the obstacle. Even showing the highest first deflection, the CDC C11 R11 3-3pt5 3-3pt5* results in an excellent return to neutral position. In other hand, the CDC as C13 R13 12-2 12-2* and C13 R13 6-3 6-3* are close to the critical damping in a large part of the maneuver, resulting in a return to the nominal position between M_s and M_u below its static position.

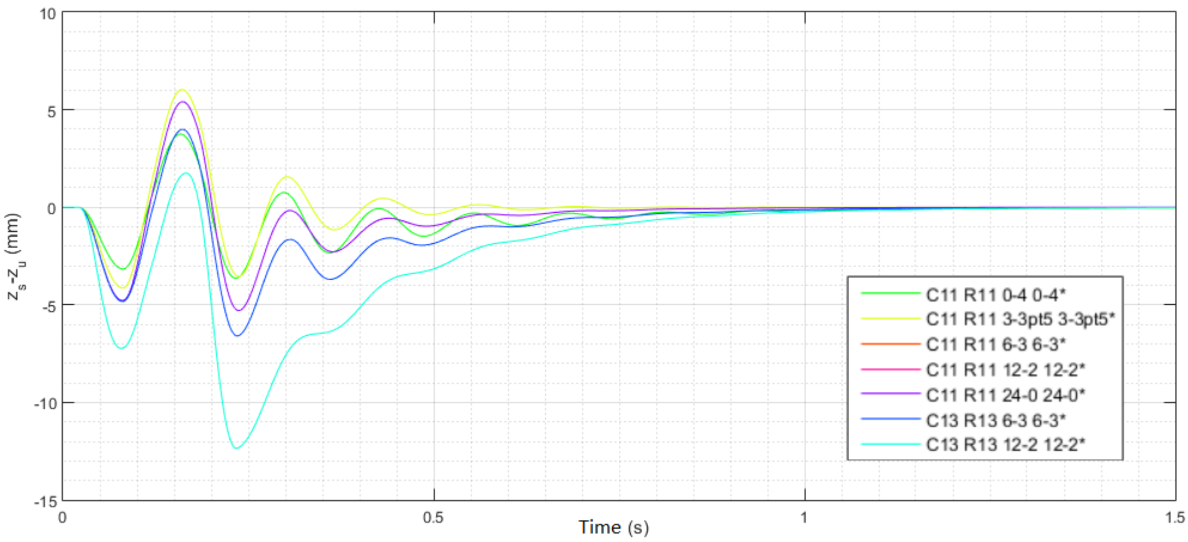

Figure 6. Time-domain comparison between the damper displacements for different CDC in a quarter-car model during a slope maneuver.

The application of a base harmonic motion input allows verifying the time window required for the system to be driven only by their homogeneous response. Furthermore, in a preliminary analysis on the Figure 7 highlighted that the damper uses only 53% of the maximum designed suspension travel during this maneuver. For almost all CDC the homogeneous response describe the system behavior satisfactorily when t> 0,37s, except for C11 R11 0-4 0-4* which takes about 0,57s. On the particular response phase, the maximum positive displacement is 6,66mm (t = 0,1488s) occurring on the CDC C11 R11 3-3pt5 3-3pt5*, and the maximum negative value is 13,50mm (t = -0,3026s) occurring on the CDC C13 R13 12-2 12 -2*. For the homogeneous response the minimum displacement occurs on the CDC C11 R11 0-4 0-4* and its value is approximately 5,77mm. In other hand, the maximum displacement occurs on the CDC C13 R13 12-2 12-2* and its value is approximately 11,68mm. On this phase, the maximum range of motion between the masses occurs on the CDC C13 R13 12-2 12-2*, reaching a value of 13.18mm. Except for the CDC C11 R11 3-3pt5 3-3pt5*, the average displacement of the others are negative, indicating that the system is not able to return the static position in this given amplitude and frequency.

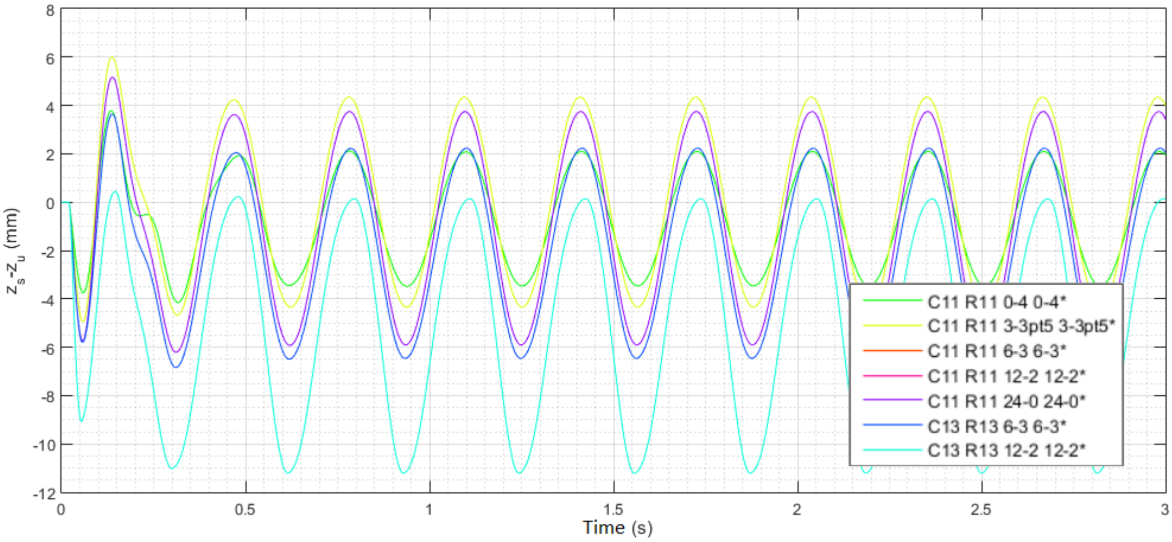

Figure 7. Time-domain comparison between the damper displacements for different CDC in a quarter car model during a sinusoidal maneuver.

The damper operation speed shown in Figure 8 defines its instantaneous damping constant and allows evaluating if the component works within the nominal range. For instance, the CDC C13 R13 12-2 12-2 * exceeds 256 mm.s^{-1} during the compression, working in a region where the component behavior is unknown. Therefore, the obtained compression speed of 376mm.s^{-1} may not be as the resulting compressions speed obtained in an identical physical experiment. The CDC C11 R11 0-4 0-4* exhibits a relatively lower compression speed when the time is less than 0.2s and is the last to satisfactorily return to the equilibrium position.

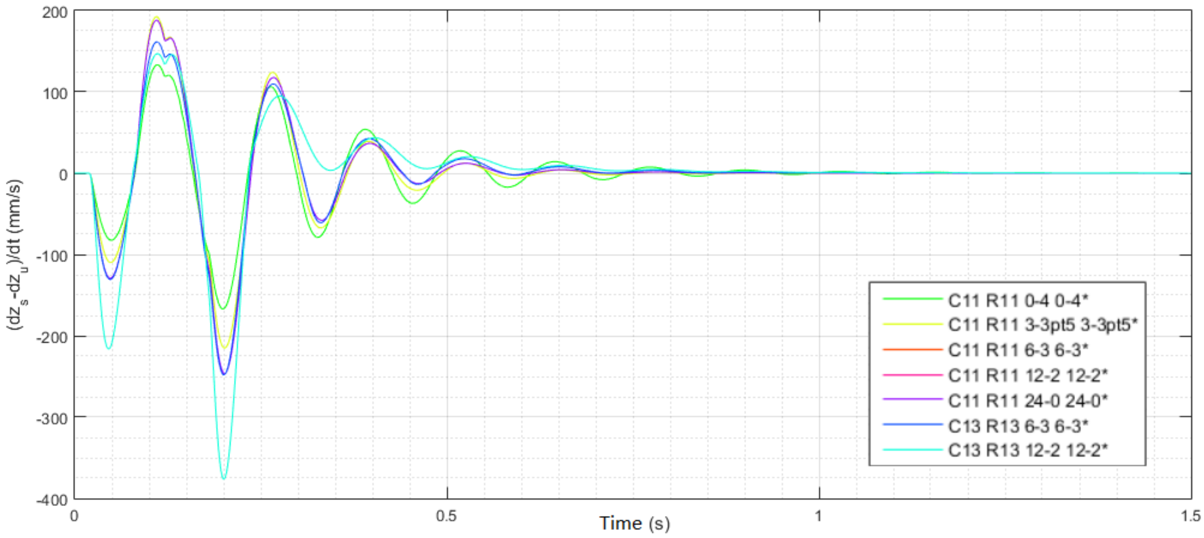

Figure 8. Time-domain comparison between the damper velocities for different CDC in quarter-car model during a slope maneuver.

During the harmonic maneuver response shown in Figure 9, only CDC that does not operate within the designed speed limit is the C13 R13 12-2 12-2 *, reaching a value of 423 mm.s^{-1} (t = 0.0316) shortly after the beginning of the obstacle. Furthermore, there is large speed gradient for all CDC, characterizing a peak region, in which the CDC C13 R13 6-3 6-3* shows the highest velocity (240mm.s^{-1}, t=0,0304s) between the components working within the operational range. During the homogeneous phase the smaller positive and negative velocities are evidenced on the CDC C11 R11 0-4 0-4*, ranging from 54.46 $mm.s^{-1}$ to 56.75 $mm.s^{-1}$. Since the curve C13 R13 12-2 12-2* should not be used on this project, the highest speeds occur in the CDC C11 R11 24-0 24-0*, ranging from 94,36 $mm.s^{-1}$ and -98.76 $mm.s^{-1}$. Again, the CDC C11 R11 0-4 0-4* has a relative delay to achieve the homogeneous phase.

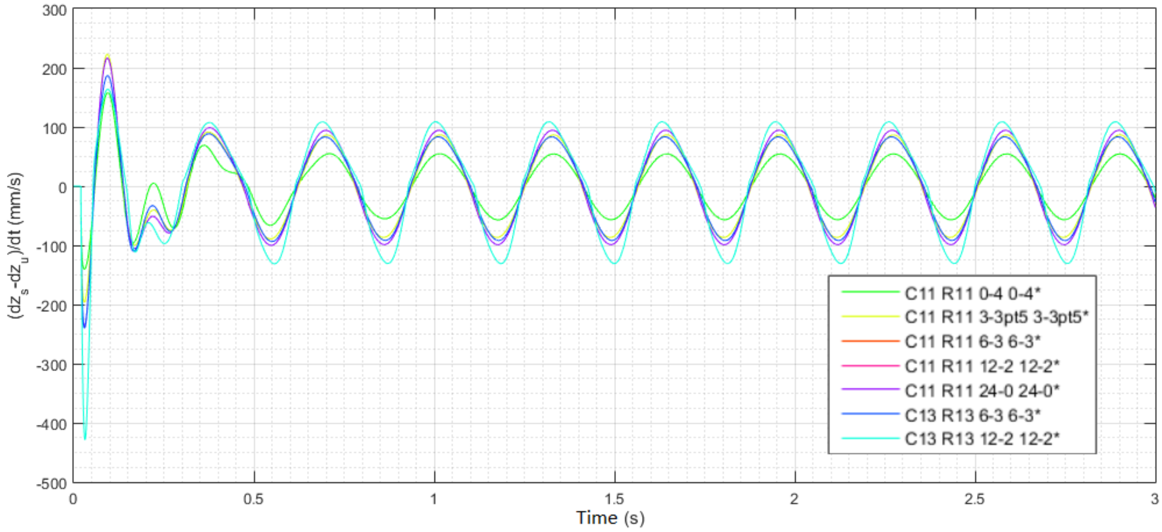

Figure 9. Time-domain comparison between the damper velocities for different CDC in quarter-car model during a sinusoidal maneuver.

Nishida (2012) states that the Corti, in the human inner ear has sensitivity to the accelerations in the three Cartesian axes, which indicates the chassis vertical acceleration as an analysis output due the fact that it is a driver perception source. High accelerations values are associated to driving discomfort and to a high fraction on the suspension response associated to the M_s motion. Vertical accelerations with large amplitude and for a substantial time can be interpreted as parasites inertial forces that hinder the stability of the vehicle and therefore compromise their overall performance.

The accelerations of the sprung mass versus time when the vehicle is subjected to the maneuver described on Equation 3 are plotted in Figure 10. Throughout the maneuver the highest values of M_s response are obtained in C11 R11 0-4 0-4* configuration, reaching a maximum negative value when the wheel is in the flat part of the obstacle (t = 0,112s), showing a peak value equal to 24.57 $mm.s^2$. The maximum positive value occurs 0.02 seconds after the wheel leave the obstacle (t = 0.2s), reaching the value of 27.18 $mm.s^2$. For all the CDC occurs a non-harmonic acceleration when the wheel gets the eccentric phase of the movement (t = 0.12 s).

The smaller accelerations occur on the CCA C13 R13 12-2 12-2*, with positive and negative maximum values of 19.00 $mm.s^2$ (t = 0,13s) and 18.94 $mm.s^2$ (t = 0,2s), respectively. However, this configuration shows a relative response delay on the subsequent fluctuations. For instance, if compared to the CDC C11 R11 0-4 0-4*, the delay of third deflection point on the positive part of the response curve for the CDC C13 R13 12-2 12-2* is 0,015s.

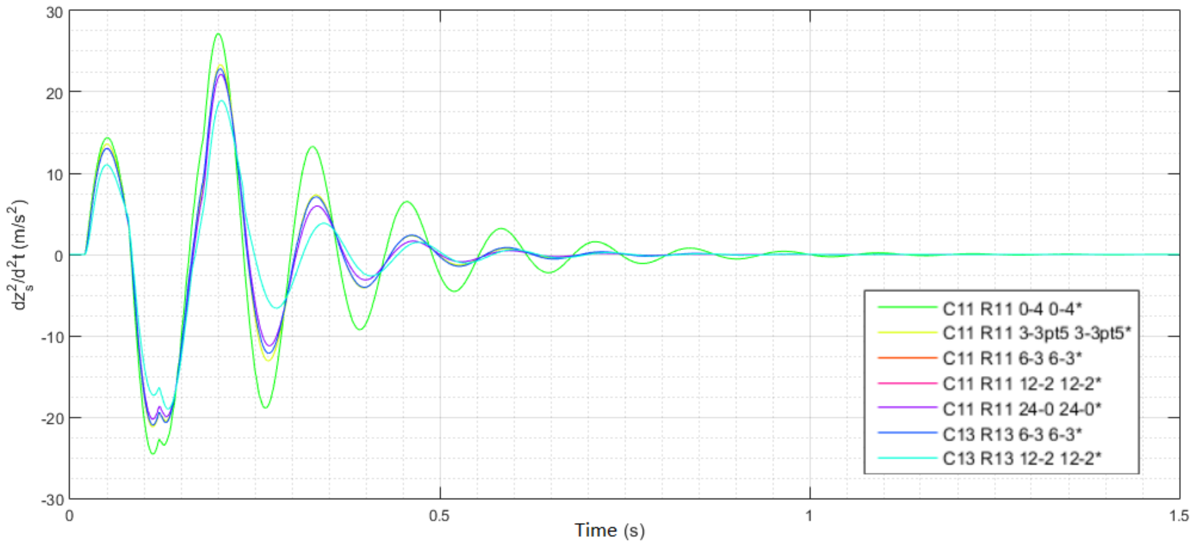

Figure 10. Time-domain comparison between the M_s (d^2Z_s)/(dt^2) for different CDC in quarter-car model during a slope maneuver.

Large accelerations on the unsprung mass are related to a larger force exerted by M_u, but the riding comfort is not directly linked to this response. Furthermore, a harmonic motion is highly desirable because it provides a better gradient of forces which enhances the system response speed since it is less dependent on the delay associated with the components inertia. The acceleration of the unsprung mass over time when the vehicle is subjected to a sinusoidal input is shown in Figure 11. In all curves M_u develops a high accelerations increment when the obstacle is introduced, reaching a peak values about 3.6 times higher than the M_s peak value. The maximum negative acceleration occurs on the CDC C11 R11 0-4 0-4* during the phase in which the system particular response has a great influence on its overall response, reaching the peak value of -29.78 mm.s^2 (t = 0,0968s). During the homogeneous phase the positive and negative maximum accelerations are very similar for all curves except the CDC C13 R13 12-2 12-2*. The maximum positive value is approximately 9,75 mm.s^2 for all the CDC, and the maximum negative value is -10,78 mm.s^2 on the CDC C13 R13 12-2 12-2*.

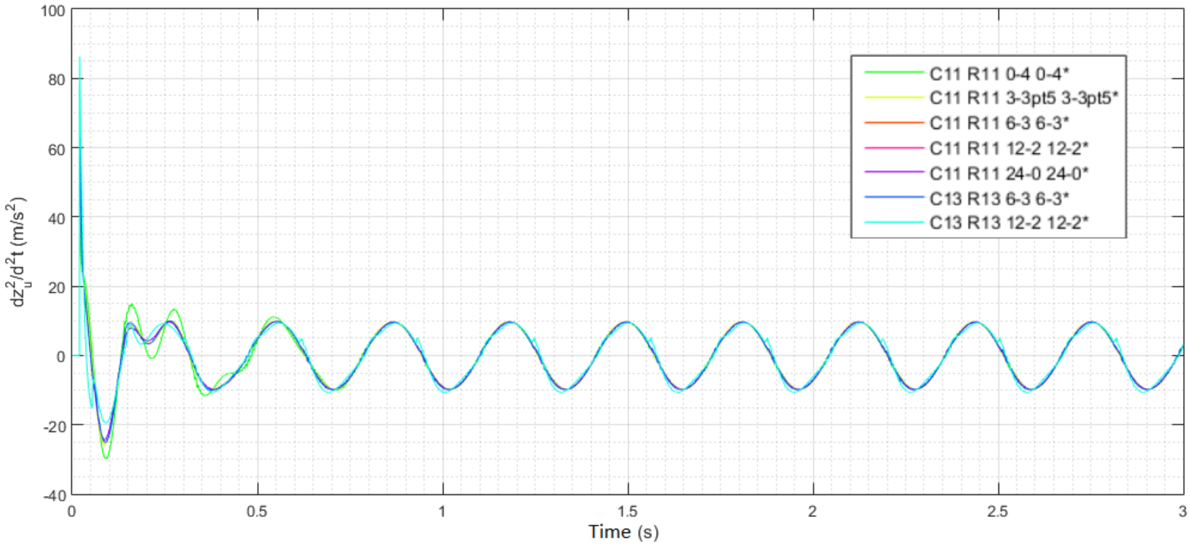

Figure 11. Time-domain comparison between the Mu (d2Zs)⁄(dt2) for different CDC in quarter-car model during a sinusoidal maneuver.

Filters are introduced in order to highlight desired output conditions. First, an exclusion condition is established, which is based on the maximum operational speed of the dampers. Furthermore, even if the maximum suspension travel design does not necessarily compromise the system performance, it is added as a second exclusion condition, since this scenario is not desirable for the project. Therefore, the main code returns a warning to the operator if one of the conditions is met. The Table 2 highlights some curves with undesirable behavior.

A non-exclusive condition is added in a second stage. This condition consists on the maximum displacement between all CDC. This maximum relative displacement is an interesting indicator of how the suspension nominal geometry can be changed. As suggested before, blocking all other variables a smaller relative displacement between the masses is desirable since it allows keeping the CG in a static position closer to the ground, thus ensuring greater lateral acceleration limit. In this case the logic function uses a small initial maximum value, replacing it if a higher value is found in any *tstep*. This analysis allows the designer numerically determine critical values, assisting on the decision-making process.

Table 2. Outputs from the numerical filters

CDC	v_lim	d_lim	CDC	Relative displacement
C21 R21 24-0 24-0	X		C11 R11 12-2 12-2*	1st
C23 R23 18-1 18-1*	X		C13 R13 18-1 18-1*	9th
C21 R21 0-4 0-4*	X	X	C23 R23 3-3pt5 3-3pt5*	22nd
C23 R23 24-0 24-0*		X	C13 R13 24-0 24-0*	23rd

3.1. Final considerations

This paper demonstrated the applicability of the quarter car model to describe the vertical behavior of the suspension system in time-domain, highlighting the importance of their theoretical construction on the decision making process due its inherent simplifications and small number of GDL. The model construction was based on the free body diagram applied on each of the masses, resulting in two ordinary first order differential equations capable of describe the isolated and relative response for each mass.

The graphical analysis is applied for a small number of characteristic curves and highlights the small usage of the suspension curse as wheel as characteristic curves that exceeds the operational velocity of the component. Furthermore, the accelerations of sprung and sprung mass allow identifying desirable outputs directly related to the overall vehicle performance. Finally, the numerical filter allows to exclude inappropriate inputs as well as to order them based on desired outputs, resulting in a robust and easy way to determine the project guidelines.

4. REFERENCES

Gillespie, T. D., 1992, "Fundamentals of vehicle dynamics". SAE - Society of Automotive Engineers, Warrandale, USA.

Smith, C., 1978, "Tune to win". Aero Publishers, Fallbrook, CA, 1978.

Haselein, B. Z. "Modelagem e análise em MATLAB de um sistema de suspensão automotiva com amortecimento não linear através do modelo *quarter car*". Trabalho de conclusão de curso. Universidade Federal de Santa Maria - UFSM, Santa Maria, RS, Brazil

Ubessi, C. B. "Análise de dirigibilidade de protótipo Formula SAE através de simulação computacional". Trabalho de conclusão de curso. Universidade Federal de Santa Maria - UFSM, Santa Maria, RS, Brazil.

Ferreira, H. T., 2003, "Determinação das frequências naturais e modos de vibrar de um veículo de dois eixos através de um programa computacional em MatLab-Simulink". 99p. Dissertação de Mestrado, Escola de engenharia de São Carlos - USP, São Carlos, Brazil.

Freitas, L. M. P., 2006, "Estudo da dinâmica vertical de uma suspensão veicular do tipo Macpherson". 139p. Dissertação (Mestrado em Engenharia Mecânica) Escola de engenharia de São Carlos – USP, São Carlos, Brazil.

Almeida, A. C. R., 2002, "Simulação e controle de um sistema de suspensão simplificado", 87p. Dissertação (Mestrado em Matemática Aplicada) Universidade Federal do Rio Grande do Sul - UFRGS, Porto Alegre, Brazil.

Fernandes, J. C. M., at all, 2015, "A quarter-car model comprising geometrical nonlinearities and asymmetrical dampers". Cobem 2015, Rio de Janeiro, RJ, Brazil.

ISO 4130:1978, 1978, "Road vehicles - Three-dimensional reference system and fiducial marks – Definitions"

Formula SAE. SAE International. Avaliable at: <http://students.sae.org/cds/formulaseries>. Last acess: December 2015.